# Hyal2 Expression in Tumor-Associated Myeloid Cells Mediates Cancer-Related Inflammation in Bladder Cancer

Paul R. Dominguez-Gutierrez, Elizabeth P. Kwenda, William Donelan, Padraic O'Malley, Paul L. Crispen, and Sergei Kusmartsev

## ABSTRACT

The increased presence of myeloid-derived suppressor cells (MDSC) and tumor-associated macrophages (TAM) in tumor tissue has been extensively reported. However, their role in the regulation of hyaluronan (HA) metabolism in the tumor microenvironment has not been established. Here we describe a novel function of tumor-associated myeloid cells related to the enhanced breakdown of extracellular HA in human bladder cancer tissue, leading to the accumulation of small HA fragments with molecular weight (MW) <20 kDa. Increased fragmentation of extracellular HA and accumulation of low molecular weight HA (LMW-HA) in tumor tissue was associated with elevated production of multiple inflammatory cytokines, chemokines, and angiogenic factors. The fragmentation of HA by myeloid cells was mediated by the membrane-bound enzyme hyaluronidase 2 (Hyal2). Increased numbers of $Hyal2^{+}CD11b^{+}$ myeloid cells were detected in the tumor tissue as well as in the peripheral blood of patients with bladder cancer. Coexpression of CD33 suggested that these cells belong to monocytic myeloid-derived suppressor cells. The HA-degrading function of Hyal2-expressing MDSCs could be enhanced by exposure to tumor-conditioned medium, and IL1β was identified as one of the factors involved in the stimulation of Hyal2 activity. CD44-mediated signaling played an important role in the regulation of HA-degrading activity of Hyal2-expressing myeloid cells, as the engagement of CD44 receptor with specific mAb triggered translocation of Hyal2 enzyme to the cellular surface and stimulated secretion of IL1β. Taken together, this work identifies Hyal2-expressing tumor-associated myeloid cells as key players in the accumulation of LMW-HA in the tumor microenvironment and cancer-related inflammation and angiogenesis.

**Significance:** This study identifies Hyal2-expressing tumor-associated myeloid cells of monocyte–macrophage lineage as contributors to hyaluronan degradation in bladder cancer tissue, leading to accumulation of inflammatory and proangiogenic low molecular weight hyaluronan fragments.

## Introduction

The tumor stroma, which is comprised of cellular and extracellular components, plays a major role in tumor growth and progression. The extracellular matrix (ECM) of tumors includes proteoglycans and glycans such as hyaluronic acid, also called hyaluronan (HA). HA is a member of the glycosaminoglycan family of polysaccharides synthesized at the cell surface and is characterized by very high molecular weights ($2 \times 10^5$ to $10 \times 10^6$ kDa) and extended lengths of 2–25 μm (1). Increased HA synthesis is associated with wound healing and tumor growth (1–2). Several cancer types including breast, prostate, brain, lung, and bladder are highly enriched with HA (2–4). Within the tumor tissue, HA buildup is frequently associated with increased degradation of HA, leading to the accumulation of low molecular weight HA (LMW-HA) fragments (5, 6). Several studies have demonstrated that LMW-HA displays unique biologic activities that are not shared by high molecular weight HA (HMW-HA; refs. 7–8). HMW-HA is antioncogenic, anti-inflammatory, and antiangiogenic, while LMW-HA promotes inflammation and tumor angiogenesis by stimulating the expression of cytokines, chemokines, and growth factors in TLR2/TLR4–dependent manner (9). Also, LMW-HA is a potent inducer of cPLA2 activity in macrophages that promote the release of arachidonic acid; a substrate for inflammation-associated lipid mediators $PGE_2$ and leukotrienes (9).

It has been shown that the progression of bladder cancer is associated with enhanced expression of hyaluronidase 2 (Hyal2) RNA in tumor tissue (10, 11). Hyal2, a member of the hyaluronidase family, is a glycosylphosphatidylinositol-linked (GPI-linked) enzyme that is anchored to the plasma membrane and is involved in the degradation of extracellular HA (12, 13). Hyal2 cleaves high molecular weight HA into intermediate size 20-kDa fragments. In addition to increased Hyal2 expression, bladder cancer tissue is frequently infiltrated with inflammatory and immune cells (14, 15). Here we demonstrate that bladder tumor–associated myeloid cells express membrane-bound enzyme Hyal2. We also show that enhanced HA degradation in human bladder cancer is accompanied by the elevated production of inflammatory cytokines/chemokines and increased production of tumor angiogenic factors.

## Patients and Methods

### Human subjects

Freshly excised bladder tumor tissue and peripheral blood from 30 patients diagnosed with urothelial carcinoma of the bladder were collected during cystectomy or transurethral resection of bladder tumor (TURBT). Samples of normal bladder tissue were collected from patients undergoing cystectomy after obtaining written informed consent. All samples were obtained according to federal guidelines

Department of Urology, University of Florida, Gainesville, Florida.

**Note:** Supplementary data for this article are available at Cancer Research Online (http://cancerres.aacrjournals.org/).

**Corresponding Author:** Sergei Kusmartsev, University of Florida, 1200 Newell Dr., Rm-R2 165, PO Box 100247, Gainesville, FL 32610. Phone: 352-273-8235; Fax: 352-273-7515; E-mail: sakus61@ufl.edu

Cancer Res 2021;81:648–57

**doi:** 10.1158/0008-5472.CAN-20-1144

and as approved by the University of Florida institutional review board (IRB).

### Reagents and culture medium

The proteinase K and Benzonase were purchased from Sigma-Aldrich. Commercial polydisperse hyaluronan samples 1M (MW 750–1,000 kDa), 700K (500–749 kDa), 500K (301–450 kDa), 200K (151–300 kDa), 10K (10–20 kDa), and 5K (<10 kDa) were obtained from Lifecore Biomedical. Biotinylated HA-binding protein (HABP) was supplied by Millipore-Sigma. Streptavidin conjugated with PE or FITC was purchased from BioLegend. The Hyaluronan ELISA Kit was purchased from R&D Systems. Hyaluronidase-2 polyclonal antibody conjugated with PE or Alexa-488 was obtained from Bioss Antibodies. All other antibodies used for immune fluorescence and flow cytometric analysis and human IL-1β ELISA kit were acquired from BioLegend. *In vitro* experiments were conducted using complete culture media consisting of RPMI1640 medium supplemented with 20 mmol/L HEPES, 200 U/mL penicillin, 50 μg/mL streptomycin (all from Hyclone), and 10% FBS from ATCC.

### Preparation of tissue slices from human normal and bladder cancer tissues

The precision-cut tissue slices, 2–4 mm in diameter and 200–300-μm thick, were produced from cancer and normal bladder tissues using a Compresstome vibratome VF-300–0Z. After cutting, tissue slices were placed into 24-well cell culture plates in complete RPMI1640 medium supplemented with 10% FBS and antibiotics and cultured at 37°C in a humidified $CO_2$ incubator. Cell viability of cultured tissue slices was tested using the Live/Dead Cell Viability Kit purchased from Invitrogen.

### Isolation of CD11b myeloid cells from peripheral blood of patients with cancer

PBMCs were isolated from patients with bladder cancer by gradient density centrifugation using Lymphoprep (Accu-Prep, 1.077g/mL). CD11b myeloid cells were purified from PBMCs by positive selection using the anti-CD11b microbeads and columns (Miltenyi Biotec). Briefly, cells were incubated with beads conjugated with anti-mouse CD11b and positively selected on LS columns. The viability of all recovered cells was 95%, as determined by Trypan blue exclusion.

### Human cancer cell lines

The human T24 bladder cancer cell line was purchased from the ATCC. Cell line was authenticated by ATCC. Tumor cells were maintained at 37°C in a 5% $CO_2$ humidified atmosphere in the complete culture medium and used at the less than 10 passages. Cell cultures were tested for *Mycoplasma* contamination using MycoProbe Mycoplasma Detection Kit (R&D Systems).

### Preparation of tumor-conditioned medium

The source of tumor-conditioned medium (TCM) was bladder cancer tissue slice cultures or cultured T24 cell line. To prepare TCM, conditioned medium was collected 2–3 days after tissue or cell culture initiation, centrifuged, aliquoted, and stored at −80°C.

### Cytokine and chemokine profiling

Human bladder cancer and normal tissue slices were cultured in a humidified $CO_2$ incubator at 37°C. For profiling of cytokines in tissue conditioned media, cell-free culture supernatants were collected and stored at −80°C. Presence of 105 proteins in supernatants was evaluated using human cytokine and chemokine XL Proteome Array Kit from R&D Systems.

### Analysis of HA produced by human bladder cancer

#### Visualization of tumor-produced HA

Cancer or normal bladder tissue slices were cultured for 7–14 days in 24-well cell culture plates in a humidified $CO_2$ incubator at 37°C to allow for the production of HA. At the end of incubation, tissue-produced HA was found settled at the bottom of the culture plate wells. To monitor and visualize accumulation of tissue-produced HA fragments on the plastic surface, the tissue slices and culture medium were removed at different time points. The empty wells were washed with warm PBS and fixed with 4% formaldehyde for 30 minutes. After fixation, plate wells were washed with PBS containing 2% FBS and incubated overnight with biotinylated HA-binding protein (3 μg/mL, Calbiochem-EMD Millipore) at 4°C (16). Next day, after washing the wells with PBS containing 2% FBS, streptavidin conjugated with fluorochrome was added to the wells and incubated for 30 minutes at 4°C. Plates were then washed with PBS and the bottoms of the wells were visualized using EVOS (Invitrogen) or Lionheart (Biotek Instruments) immunofluorescent imaging microscopes.

#### Evaluation of HA size

HA size analysis was determined using PAGE as described previously (17). Briefly, conditioned medium from cancer and normal bladder cancer tissue slices were centrifuged, aliquoted, and stored at −80°C. To prepare samples for HA size analysis, thawed samples were digested with proteinase K to remove proteins, benzonase for the depletion of nucleic acids (RNA, DNA), and ethanol to extract lipids was added. Samples along with HA standards were then subjected for PAGE. The tissue-produced HA was visualized on the gel by staining with "Stains All" dye (Sigma-Aldrich).

### Immunofluorescent microscopy and flow cytometry

Immunofluorescent staining and flow cytometry analysis was performed as described previously (18, 19). Image analysis was done using Gen 5 Prime v 3.08 software (Biotek Instruments). Flow cytometry data and microscope pictures showed are representative of at least two separate determinations.

### Western blotting

Cells were lysed in M-PER Mammalian Protein Extraction Reagent (Thermo Scientific) containing protease and phosphatase inhibitors. Whole-cell lysates (30 μg/lane) were subjected to 10% SDS-PAGE and blotted onto polyvinylidene difluoride membranes. Membranes were blocked for 1 hour at room temperature with 5% dry skimmed milk in TBS (20 mmol/L Tris-HCl, pH 7.6, 137 mmol/L NaCl plus 0.1%, v/v, Tween 20) and probed with appropriate primary antibodies overnight at 4°C. Membranes were washed and incubated for 1 hour at room temperature with secondary antibody conjugated with HRP. Results were visualized by chemiluminescence detection using a SuperSignal West Pico substrate (Thermo Scientific). To confirm equal loading membranes were stripped using Restore Western Blot Stripping Buffer (Thermo Scientific) and reprobed with an antibody against β-actin (Santa Cruz Biotechnology, Inc).

### Statistical analysis

The statistical significance between values was determined by the Student *t test*. All data were expressed as the mean ± D. Probability values ≥ 0.05 were considered nonsignificant.

## Results

### Enhanced HA degradation in bladder cancer tissue results in the accumulation of LMW-HA fragments

Normal bladder tissues produced predominantly long, structured linear pericellular HA (**Fig. 1A**), whereas the bladder cancer samples generated highly fragmented tissue-associated HA (**Fig. 1B**). The size of HA secreted by normal and bladder cancer tissues was further characterized by gel electrophoresis. Interestingly, tissues from normal bladder tissues (**Fig. 2A**, left) produced mostly HMW-HA (150 kDa and higher) with undetectable levels of LMW-HA. In contrast, the human bladder cancer tissues generated fragmented HA with a prevalence of LMW-HA with MW < 20 kDa (**Fig. 2A**, right) confirming our prior observation of increased HA fragmentation in bladder cancer tissues (**Fig. 1B**).

### Enhanced HA degradation in tumor tissue is associated with elevated secretion of inflammatory, angiogenic, and tumor-supporting factors

Accumulating evidence suggests that HA fragments with low molecular weight can directly promote tumor progression by stimulating the secretion of various factors that enhance tumor migration, invasion, inflammation, and angiogenesis. (5, 6, 9). To assess and compare the cytokine profile produced by normal and bladder cancer tissues, we analyzed the TCM collected from normal and bladder cancer organoid tissue slices for the presence of 105 cytokines and chemokines using proteome multiplex assay. Our data demonstrate that in contrast to normal tissue, the bladder cancer tissue secretes higher levels of various biologically active factors (**Fig. 2B**; Supplementary Figs S1, S2A, and S2B). Among them, we detected several angiogenic factors: VEGF, angiopoietin-2, angiogenin, HGF, and thrombospondin; multiple chemokines and growth factors associated with inflammation and recruitment of different cell subsets to the tumor site such as CXCL1 (GRO-alpha), CCL2 (MCP1), G-CSF, CCL7 (MCP3), CXCL5 (ENA-75), CXL11 (I-TAC), FLT3, and lipocalin-2. The bladder cancer tissues also produced proteins involved in immune regulation (IL6, IL8, osteopontin, IL11, IL17A IL18Bpa, TIM-3, IL1ra) and tissue remodeling (MMP-9, chitinase3-like1, IGFBP-2, uPAR, thrombospondin). Proteins implicated in tumor cell invasion and migration, such as DKK1 PAI-1 (Serpin-E1) and HGF, were also prevalent in cancer tissue. Combined data for the production of proteins by normal and cancer bladder tissues were presented as a heatmap (Supplementary Fig. S2A and S2B). Taken together, these data suggest that the accumulation of LMW-HA fragments within bladder cancer is accompanied by elevated production of multiple bioactive factors that are associated with tumor growth and progression.

### Detection of Hyal2-expressing tumor-associated myeloid cells in human bladder cancer

Increased levels of inflammatory chemokines and cytokines produced by the tumor facilitate cancer-associated inflammation and drive recruitment of myeloid cells to the tumor microenvironment where they become involved in bidirectional crosstalk with tumor cells (20, 21). As shown in **Fig. 3A**, bladder cancer tissue is infiltrated with myeloid cell subsets when compared with normal bladder tissue. Moreover, the tumor-infiltrating cells are frequently associated with enhanced HA fragmentation (**Fig. 3B**; Supplementary Fig. S3). We hypothesized that the enhanced HA degradation within bladder cancer might be attributed to the presence and activity of tumor-recruited myeloid cells, which abundantly present in bladder tumor tissue

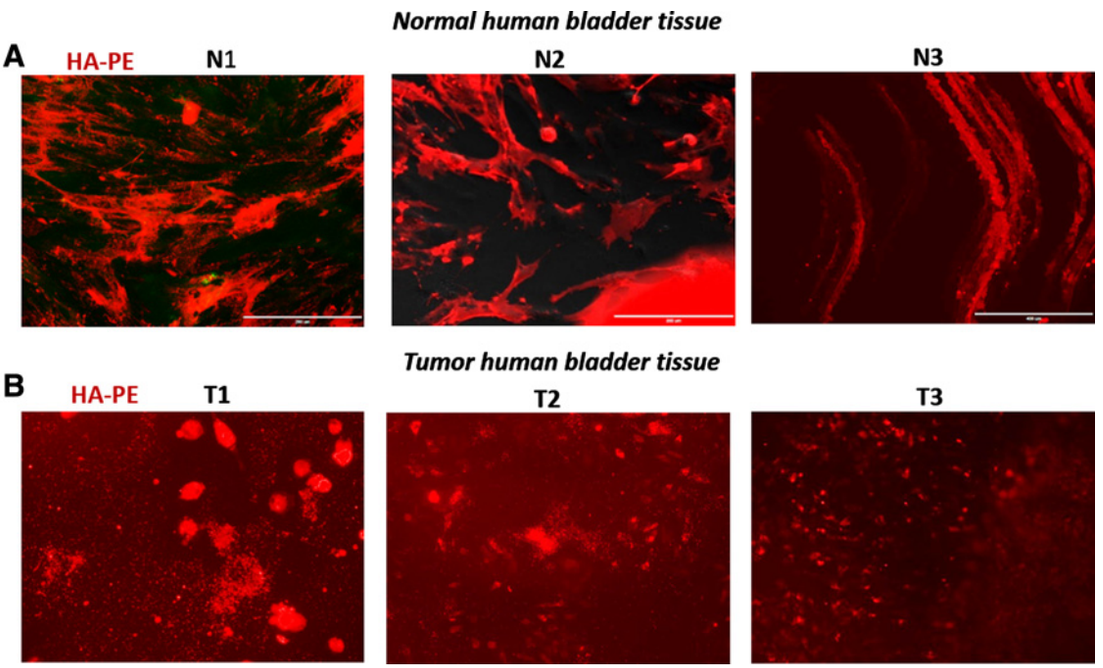


**Figure 1.**

Visualization of HA produced by the tumor and normal human bladder tissue slices. Representative images showing tissue-produced HA in normal and tumor bladder tissues. Tissue slices prepared from normal (**A**) and tumor (**B**) human bladder tissue were cultured in complete medium in 24-well plates for 7 days. After removing culture medium and tissue slices, plates were fixed with 4% formaldehyde and stained for HA (red). The expression of HA was evaluated using immunofluorescent microscopy.

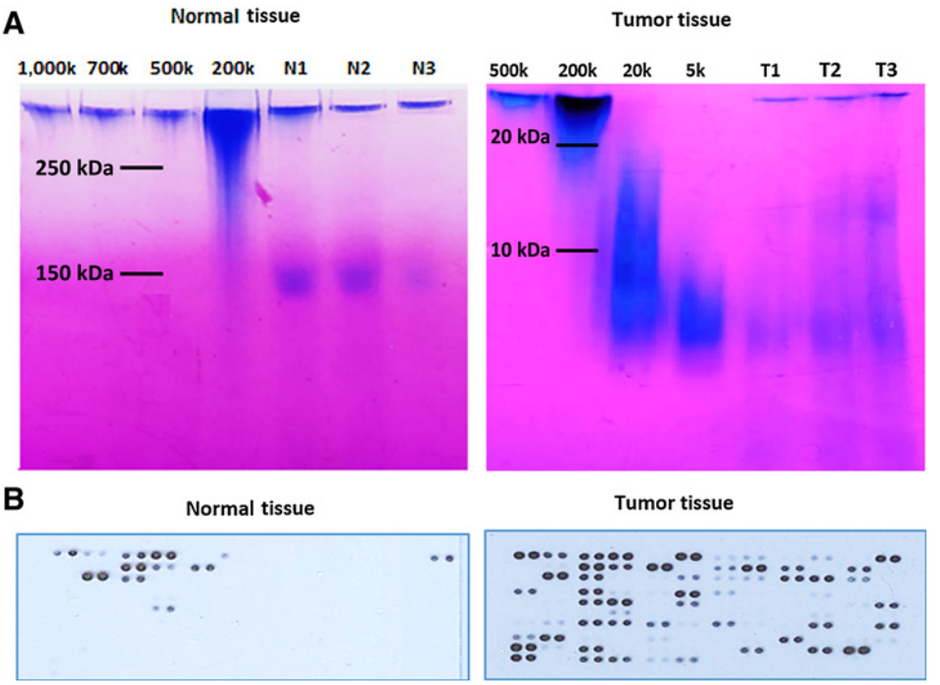


**Figure 2.**
Enhanced HA degradation, accumulation of LMW-HA, and elevated production of cytokines/chemokines in human bladder cancer tissue. Precision-cut tissue slices were prepared from freshly obtained normal and tumor human bladder tissue pieces and cultured in 24-well plates in the complete culture medium. Cell-free supernatants were collected on days 5–7 and stored at −80°C until analysis of tumor-produced HA using PAGE (**A**) and cytokines/chemokine antibody arrays (**B**).

(**Fig. 3C**). To test this hypothesis, we costained HA produced by bladder cancer tissue slices with common myeloid cell marker CD11b. As shown in **Fig. 3D** and Supplementary Fig. S3, the myeloid cells localized nearby and some adhered to highly degraded HA fragments. Hyal2 is an enzyme responsible for HA degradation in the tumor microenvironment, whose increased expression in progressive bladder cancer was recently reported (11). Hence, we stained cancer tissue samples for the HA, Hyal2, and CD11b. Data presented in **Fig. 3E**; Supplementary Fig. S4 demonstrate the presence of Hyal2-expressing cells in tumor-bladder tissue slice cultures among both adherent and nonadherent cell fractions. Moreover, Hyal2 expression was observed in areas with highly fragmented HA and associated with a subset of tumor-infiltrating CD11b myeloid cells (**Fig. 3F**), suggesting a possible contribution of these cells to the enhanced HA degradation in bladder cancer tissue.

### Hyal2-expressing myeloid cells in peripheral blood of patients with cancer

The peripheral blood of patients with bladder cancer contains increased numbers of myeloid cells, including granulocytic, and monocytic myeloid-derived suppressor cells (MDSC) as compared with healthy individuals (22). To explore whether Hyal2-expressing myeloid cells could be also detected in peripheral blood, we isolated the CD11b$^+$ cell populations from peripheral blood of patients with bladder cancer and healthy donors and stained with anti-Hyal2 Abs. Data presented in **Fig. 4A** and Supplementary Fig. S5A and S5B indicate that myeloid cells from the blood of patients with cancer contain significantly more Hyal2-positive cells as compared with healthy individuals. Additional analysis revealed that blood-derived Hyal2$^+$ cells show mononuclear morphology (Supplementary Fig. S6) and also express a marker of monocytic MDSCs CD33, as well as CCR2 receptor, M-CSF receptor (CD115), and GM-CSF receptor (CD16; Supplementary Fig. S7A and S7B).

We also found that exposure of myeloid cells to TCM further stimulated the expression of Hyal2 (**Fig. 4B**), suggesting that expression of this enzyme could be upregulated in myeloid cells upon recruitment to the tumor microenvironment with an abundance of tumor-derived factors. Furthermore, a significant portion of Hyal2$^+$ myeloid cells also coexpressed the antigen-presenting cell marker HLA-DR (**Fig. 4C**): 13.7% in nonstimulated versus 46.7% in TCM-stimulated CD11b myeloid cells. Interestingly, that expression of Hyal2 was detected in mostly dispersed granular form with intracellular localization in the cytoplasm (**Fig. 4D**; Supplementary Fig. S7A). However, engagement of cells with antibodies against CD44 promoted significant changes in both cellular shape and Hyal2 localization (**Fig. 4E**), supporting the idea that the CD44 receptor is involved in the regulation of Hyal2 function (12, 13, 23, 24).

### IL1β stimulates HA-degrading activity of Hyal2$^+$ myeloid cells

To examine whether TCM-stimulated CD11b$^+$Hyal2$^+$HLA-DR$^+$ cells are functionally active, we tested their HA-degrading activity. To this end, we added the CD11b cells isolated from peripheral blood of patients with cancer to the culture plates precoated with commercial HA (MW 200 kDa), and cultured cells in the presence of TCM for 10 days. The visualization of HA was executed using biotinylated hyaluronan-binding protein (HABP). As shown in **Fig. 5A** (right), TCM-stimulated myeloid cells were able to promote the degradation of extracellular HA. Furthermore, by end of the culture (10 days), most of the TCM-stimulated myeloid cells acquired the shape of mature APCs and were able to internalize the fragmented HA (**Fig. 5B**). We next examined the potential cytokines/factors that could be involved in the stimulation of HA-degrading activity mediated by Hyal2-expressing myeloid cells. Hyal2$^+$ cells were isolated from peripheral blood of patients with cancer and cultured in the presence or absence of the following: human recombinant GM-CSF, M-CSF, IL1β, osteopontin, or TCM. The HA-degrading activity of cultured Hyal2$^+$ cells was evaluated by the visualization of degraded HA using IF microscopy (**Fig. 5C**), and quantification of small HA fragments detected on a plastic surface in cell culture plates using imaging software (**Fig. 5D**). Obtained data demonstrate that only IL1β among tested cytokines has

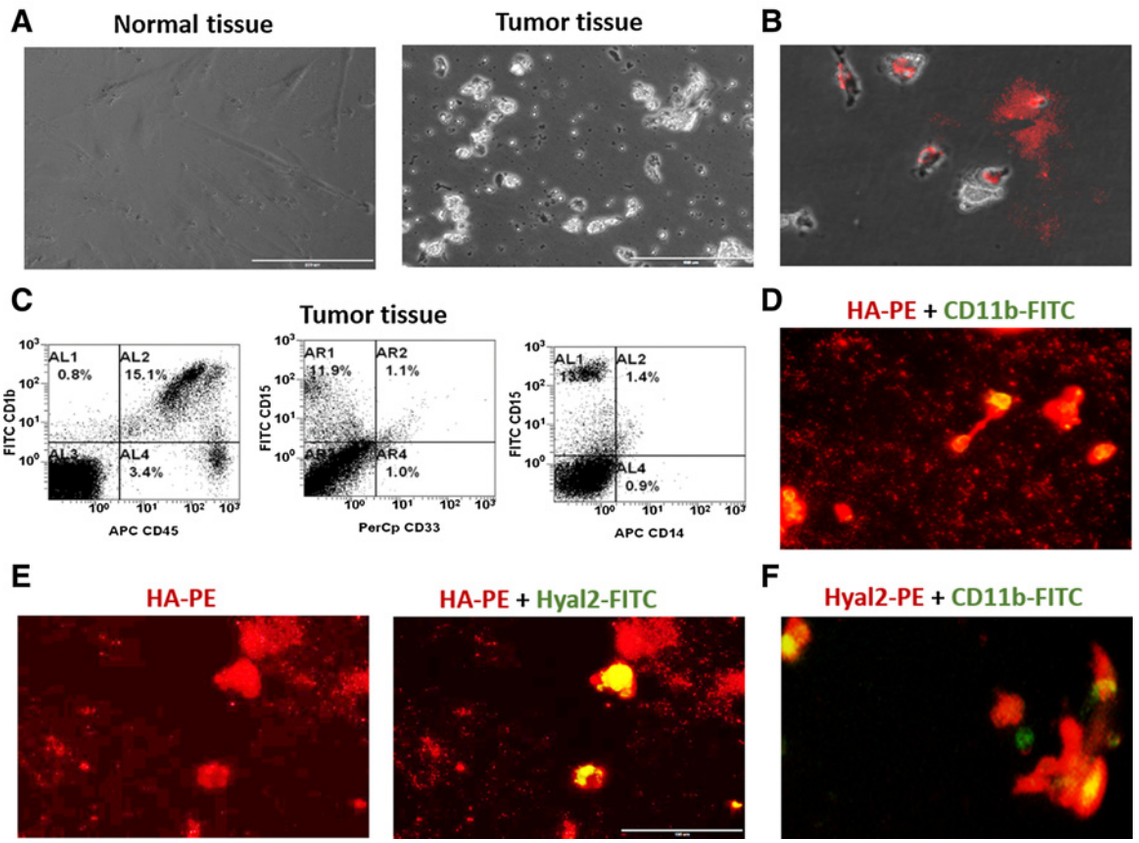


**Figure 3.**

Degradation of HA in human tumor tissue is associated with the presence of tumor-infiltrating CD11b$^+$Hyal2$^+$ myeloid cells. **A**, Representative bright-field images of normal bladder tissue (left) and bladder cancer tissue (right) from the same patient are shown. **B,** Colocalization of tumor-infiltrating cells and fragmented tumor-produced HA (red). A representative image is shown. **C,** Flow cytometric analysis of bladder cancer tissue. Tumor tissue from cancer patients was digested with a collagenase cocktail to prepare single-cell tumor suspension. The single-cell suspension was costained with CD11b-FITC, CD45-APC, CD33-PerCp, CD15-FITC, CD14-APC antibodies, and analyzed by flow cytometry. Representative images are shown. **D,** Colocalization of tumor-infiltrating CD11b myeloid cells and fragmented tumor-produced HA. Representative image of CD11b (green) and HA (red) in bladder cancer tissue is shown. **E,** Visualization of tumor-produced HA and tumor-associated Hyal2-expressing cells. The human cancer tissue slices were cultured for 5 days. Nonadherent cells were carefully removed, washed with PBS, and fixed with 4% formaldehyde. To visualize the tumor-produced HA, biotinylated HA-binding protein and PE-labeled streptavidin were subsequently added. Representative images of HA (red) and Hyal2 (green) are shown. **F,** Detection of tumor-infiltrating CD11b$^+$Hyal2$^+$ myeloid cells. Representative image of CD11b (green) and Hyal2 (red) in bladder cancer tissue is shown.

been able to promote strong HA-degrading activity in Hyal2$^+$ myeloid cells. The knockdown of the Hyal2 gene in blood-derived myeloid cells led to the reduced ability of those cells to degrade extracellular HA (Supplementary Fig. S8). A recently published study demonstrated that IL1β can be produced by macrophages in a CD44-dependent manner (25). Indeed, data presented in Supplementary Fig. S9A and S9B indicate that incubation of CD11b myeloid cells, isolated from peripheral blood of patients with cancer, with anti-CD44 antibodies promoted the IL1β secretion.

### Bone marrow as a source of Hyal2-expressing cells

Further analysis of myeloid cells obtained from peripheral blood of patients with bladder cancer revealed that Hyal2-positive cells did not express the monocytic marker CD14 (**Fig. 6A**). Long-term culture of Hyal2$^+$ cells showed that these cells retained the antigen-presenting cell marker HLA-DR, but the expression of Hyal2 becomes somewhat weaker and its localization was more intracellular overtime (**Fig. 6B**). Importantly, the HLA-DR$^+$CD11b$^+$ cells and Hyal2$^+$HLA-DR$^+$ myeloid cells can be detected in bladder cancer tissue (**Fig. 6C** and **D**, respectively) near areas that enriched for highly fragmented HA (**Fig. 6D**, right image), suggesting the contribution of this myeloid cell subset to the process of HA degradation in the tumor microenvironment. Finally, taking into consideration that the primary location in the body where myelopoiesis takes place is bone marrow, we hypothesized that bone marrow may potentially serve as a source of Hyal2$^+$ myeloid cells. Analysis of CD11b myeloid cells, isolated from normal human bone marrow, confirmed the significant presence of Hyal2-expressing myeloid cells in bone marrow (**Fig. 6E** and **F**). Together, these data demonstrate that Hyal2-expressing myeloid cells can be detected in bladder cancer tissue, close to the HA degradation points.

## Discussion

HA is a major component of the extracellular and pericellular matrix, which supports the normal tissue homeostasis. Deregulated

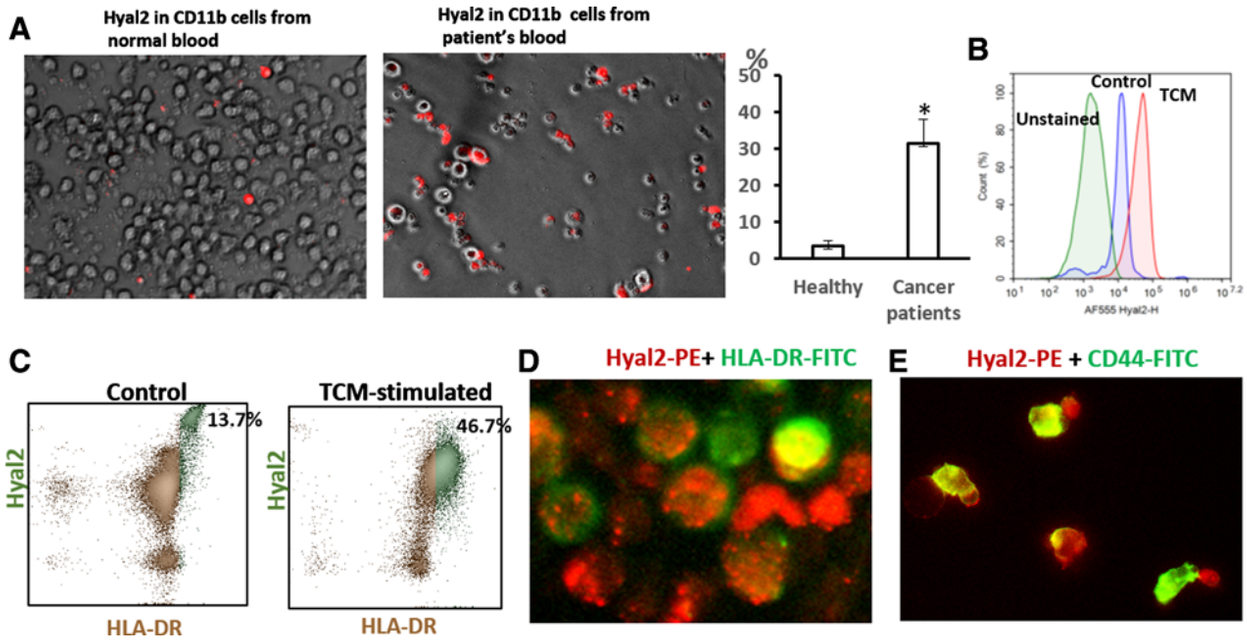


**Figure 4.**

Identification of Hyal2-expressing myeloid cell subsets in peripheral blood from patients with bladder cancer. **A,** Upregulated expression of Hyal2 by peripheral blood-derived CD11b myeloid cells from patients with cancer. CD11b myeloid cells were isolated from the peripheral blood of normal individuals or cancer patients using magnetic beads, stained with anti-Hyal2-PE antibodies, and analyzed by immunofluorescent microscopy. The percent of Hyal2+ cells was evaluated using an immunofluorescent imaging microscope. Average means ± SD are shown. *, $P < 0.05$. **B** and **C,** Analysis of Hyal2 expression in blood-derived myeloid cells using flow cytometry. CD11b myeloid cells were isolated from the peripheral blood of patients with cancer and cultured in complete culture medium for 48 hours in the presence or absence of TCM. T24 tumor cell–derived culture supernatant was a source of TCM in these experiments. Collected cells were washed with PBS and stained with anti-Hyal2 Abs (**B**), anti-Hyal2, and anti-HLA-DR abs (**C**). The expression of indicated markers was measured using flow cytometry. Representative images are shown. **D,** Analysis of Hyal2 localization in TCM-stimulated myeloid cells using immunofluorescent microscopy. TCM-stimulated myeloid cells were prepared as indicated above and stained with anti-Hyal2-PE (red) and HLA-FITC (green) antibodies. Representative images are shown. **E,** Hyal2$^+$ myeloid cells coexpress CD44. CD11b myeloid cells were isolated from the peripheral blood of patients with cancer using magnetic beads. TCM-stimulated myeloid cells were prepared as indicated above and stained with CD44-FITC and anti-Hyal2-PE. A representative image is shown.

HA metabolism has been observed in the bladder, prostate, breast, brain, lung, and other cancers. These cancers are characterized by elevated levels of HA and increased HA fragmentation in tumor tissue due to enhanced activity of hyaluronidases. Accumulating evidence suggests that HA fragments with LMW-HA directly stimulate the secretion of various factors that promote tumor progression. However, the underlying mechanisms of increased HA degradation within the tumor microenvironment are not fully understood. Herein, we evaluated HA metabolism in bladder cancer samples obtained from patients undergoing surgical resection. Our analysis revealed that normal human bladder tissue produced HMW-HA, low levels of cytokines, and contained negligible inflammatory and immune infiltrates. In contrast, bladder cancer tissues displayed strong HA degradation resulting in the accumulation of LMW-HA fragments and elevated production of chemokine, cytokines, and angiogenic factors.

The molecular weight and size of HA fragments are important for the biological activity mediated by HA. HMW-HA is antioncogenic (7, 8) and anti-inflammatory (26). In naked-mole rats, which display exceptional cancer-free longevity and a lifespan exceeding 30 years, extremely high molecular mass HA was found (7). This HMW-HA accumulates abundantly in naked mole-rat tissues due to decreased activity of HA-degrading enzymes and a unique sequence of HA-producing enzyme hyaluronan synthase 2 (*HAS2*). Once HMW-HA was removed by knocking down HAS2 or overexpressing the HA-degrading enzyme, Hyal2, naked mole-rat cells became susceptible to malignant transformation and readily formed tumors in mice. In stark contrast to HMW-HA, LMW-HA was shown to exert tumorigenic functions such as stimulation of cancer-related inflammation, tumor angiogenesis, and metastasis. Inflammation plays a critical role during different steps of tumor development and progression. Immune cells infiltrate tumors, creating an inflammatory microenvironment in which an extensive interaction -between immune cells and tumor cells takes place. LMW-HA fragments contribute to cancer-related inflammation by stimulating cytokine/chemokine production in a TLR2- and TLR4-dependent manner in both immune and tumor cells (9, 27–29). Furthermore, it was shown that degraded HA products with specific sizes of 4–25 disaccharides (MW ∼ 0,5–3,0 kDa) exert strong angiogenic activity (30). More recent studies have supported this finding (31, 32) by showing that CD44 and RHAMM-mediated signaling pathways are involved in HA-mediated angiogenesis. In addition, several studies demonstrated that LMW-HA fragments have prometastatic properties (33, 34).

In this study, we demonstrate that myeloid cells in patients with bladder cancer express the HA-degrading enzyme Hyal2. Membrane-bound enzyme Hyal2 exists as a glycosylphosphatidylinositol (GPI)-linked protein exposed to the extracellular milieu (12, 13, 35, 36). It has been proposed that Hyal1 and Hyal2 are major mammalian hyaluronidases in somatic tissues and that they act in concert to degrade HMW-HA to LMW-HA (37–39). 20-kDa

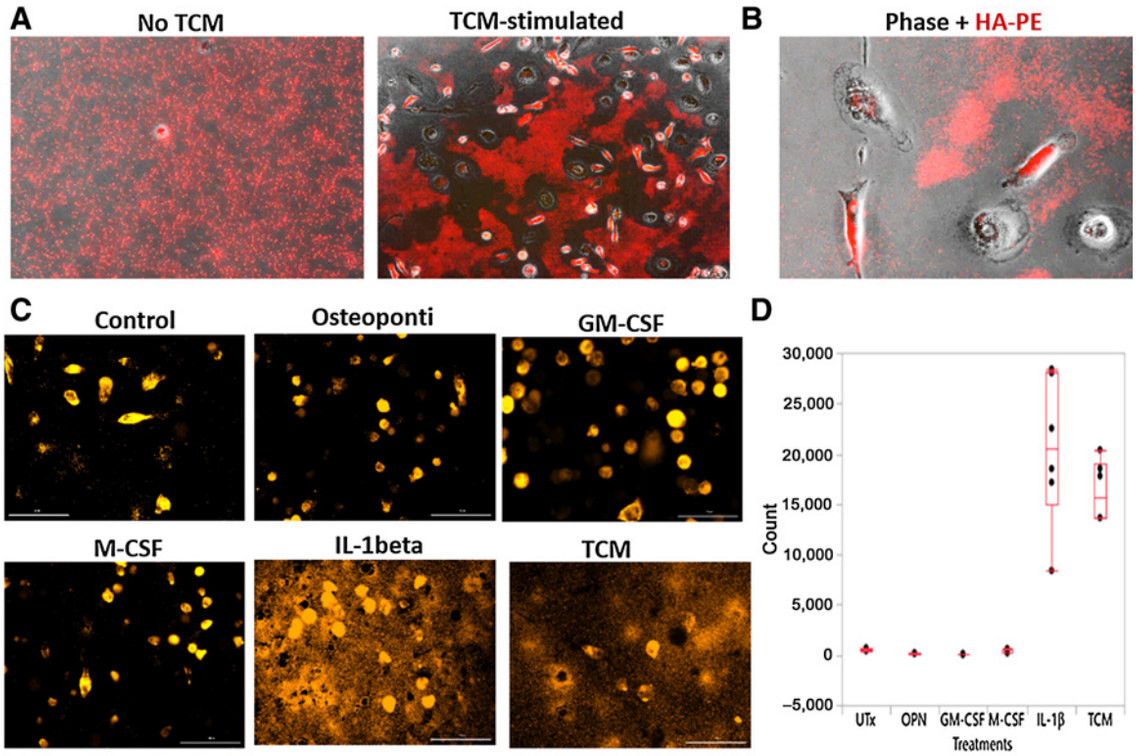


**Figure 5.**

IL1β stimulates HA-degrading activity of Hyal2$^+$ myeloid cells. **A,** Stimulation of peripheral blood-derived myeloid cells with TCM promotes the degradation of extracellular HA. Twenty-four–well cell culture plates were precoated with sterile commercial HA (MW 200 kDa). CD11b myeloid cells isolated from peripheral blood of patients with cancer were cultured in the absence (left) or the presence of TCM (right). On day 10, cell cultures were fixed with 4% formaldehyde and stained for the HA (red). Representative images of control and TCM-treated myeloid cells cultured with HA are shown. **B,** Detection of intracellular HA in TCM-stimulated myeloid cells. CD11b myeloid cells isolated from peripheral blood of patients with bladder cancer were added to the wells with precoated commercial HA. Cells were cultured in the presence of TCM for 10 days. A representative image is shown. **C,** IL1β stimulates the HA-degrading activity of Hyal2$^+$ myeloid cells. Hyal2$^+$ were directly from peripheral blood of the cancer patient and were cultured in a 24-well plate that was precoated with commercial HA (MW 200 kDa) in complete culture medium in presence of bladder TCM, or GM-CSF (50 ng/mL), M-CSF (50 ng/mL), osteopontin (OPN; 50 ng/mL), IL1β (50 ng/mL) or none (Utx). Supernatant from the patient's bladder tumor tissue culture was a source of TCM in these experiments. HA was visualized on day 10 as described in Materials and Methods using immunofluorescent microscopy. **D,** Quantification of HA fragments in cytokine-treated Hyal2$^+$ cells. Image analysis was done using Gen 5 Prime v 3.08 software (Biotek Instruments).

intermediate-size HA fragments generated by the Hyal2 near the cell surface can be transported intracellularly and delivered to lysosomes, where Hyal1 further degrades the 20-kDa to the LMW-HA fragments (< 5–10 kDa). Indeed, our observations support this model since the majority of tumor-infiltrating or peripheral blood-derived Hyal2-expressing myeloid cells exposed to the HA in the presence of activating factors (such as TCM or IL1β) efficiently engulf the HA fragments and show the presence of the intracellular HA. Without activating stimuli, the Hyal2-expressing myeloid cells show very little HA-degrading activity (**Fig. 5C** and **D**). These data suggest that Hyal2 plays a role in the rate-limiting enzyme, which upon activation with specific stimuli initiates degradation of the extracellular HA. Once degraded HA is internalized by myeloid cells, the intracellular lysosomal Hyal1 further breakdowns the engulfed HA into smaller fragments with lower molecular weight. Significant amounts of LMW-HA fragments also were detected in extracellular space of bladder cancer tissue (Supplementary Fig. S3), suggesting that both intracellular and extracellular small HA fragments could be potentially involved in pathogenic LMW-HA–mediated signaling that stimulates the enhanced production of inflammatory and angiogenic factors detected in tumor tissue.

In addition to cancer, Hyal2 has also been implicated in the pathogenesis of inflammatory joint diseases including rheumatoid arthritis and osteoarthritis. It was found that the expression of Hyal2 in patients with arthritis is significantly upregulated (40). Moreover, the expression of Hyal2 in chondrocytes can be stimulated by IL1β (41). Our data also support the direct role of IL1β in the stimulation of Hyal2-mediated HA degradation. IL1β is abundant in the tumor microenvironment and produced mostly by tumor-associated macrophages in response to the soluble CD44 (25). A recent study demonstrated that IL1β supports both tumor progression and metastasis development (42). Orthotopic injection of murine mammary cells in IL1β knockout mice led to initial tumor growth but resulted in subsequent tumor regression and prevention of metastasis development. Moreover, treating mice first with anti-IL1β antibodies followed by anti-PD1 antibodies completely abrogated tumor progression.

Some aggressive epithelial tumor cells show a high expression of Hyal2 and able to degrade extracellular HA (8). However, Western blotting analysis showed relatively weak expression of Hyal2 in human

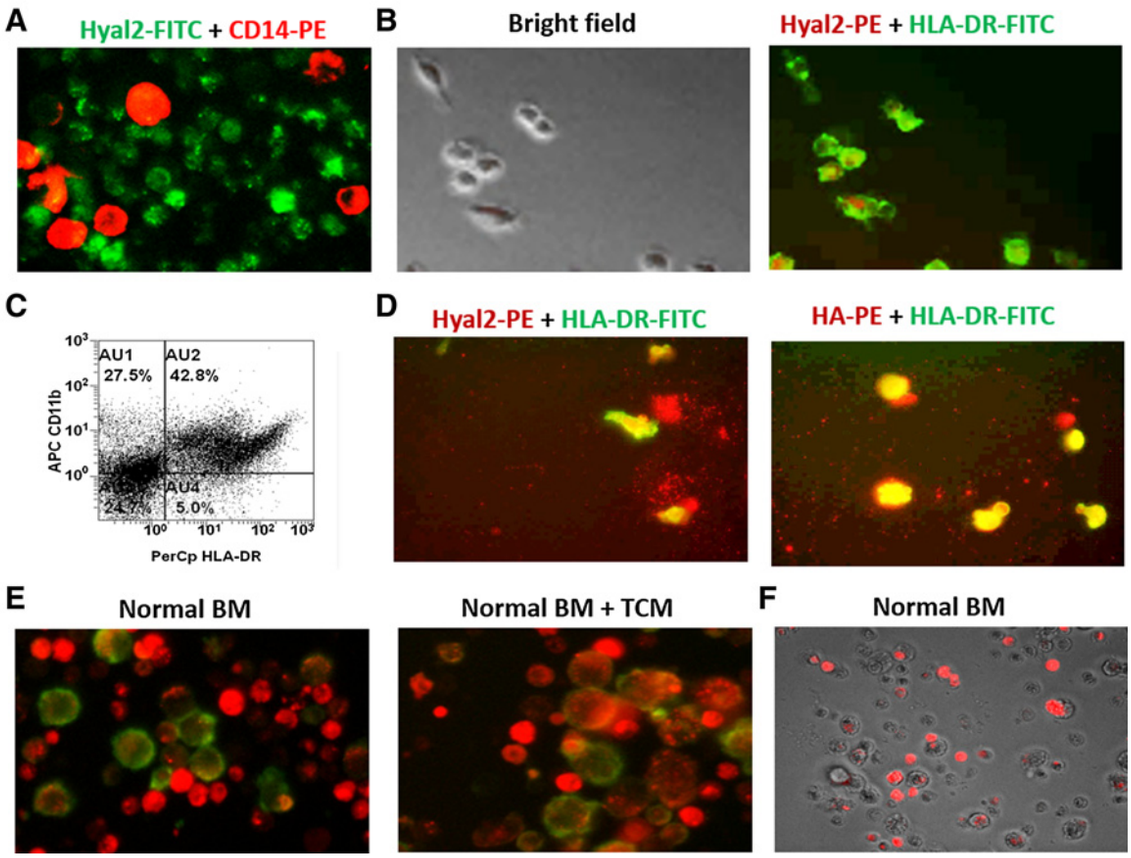


**Figure 6.**

Bone marrow as a source of Hyal2-expressing cells. **A,** Hyal2 is not associated with CD14$^+$ monocytes. CD11b myeloid cells were isolated from the peripheral blood of patients with bladder cancer with magnetic beads and stained with antibodies against CD14 (red) and anti-Hyal2 (green). A representative image is shown. **B,** TCM drives the development of Hyal2$^+$HLA-DR$^+$ cells using magnetic beads. CD11b myeloid cells were isolated from the peripheral blood of patients with bladder cancer and cultured in the presence of TCM in the complete culture medium. On day 10, plates were washed with PBS, then fixed and stained with fluorochrome-conjugated antibodies against Hyal2 (red) and HLA-DR (green). Representative images are shown. **C,** Analysis of tumor-associated CD11b, HLA-DR–expressing cells using flow cytometry. Tumor tissue from patients with bladder cancer was digested with a collagenase cocktail to prepare single-cell tumor suspension. The prepared cell suspension was costained with fluorochrome-conjugated antibodies against CD11b and HLA-DR and analyzed using flow cytometry. A representative image is shown. **D,** Detection of tumor-infiltrating Hyal2$^+$HLA-DR$^+$ cells. Twenty-four-well plates with human bladder cancer tissue slices were prepared for analysis of tumor-produced HA as described in Materials and Methods. Representative images of HA-PE (red) adherent HLA-DR$^+$ cells (green) are shown. **E,** Hyal2$^+$ myeloid cells are enriched in the bone marrow. CD11b myeloid cells were isolated from human normal bone marrow using magnetic beads. Nonstimulated (left) or TCM-stimulated (right) myeloid cells were prepared as indicated above and stained with anti-Hyal2-PE and HLA-DR-FITC antibodies. Representative images are shown. **F,** Hyal2-positive cells (red) shown in nonstimulated bone marrow. Representative image is shown.

bladder cancer cell lines (Supplementary Fig. S10). Myeloid cells, including TAMs and MDSCs, represent a major cellular component in tumor tissues that play a key role in tumor development and progression (reviewed in 20–22). Recruitment of myeloid cells to the tumor microenvironment is a constant process fueled by the increased secretion of chemokines by both malignant as well as by stromal cells, which causes the mobilization of bone marrow–derived myeloid cell precursors from bone marrow and extravasation from the circulation into the tumor. Because of a tolerogenic cytokine milieu in the tumor microenvironment, recruited myeloid cells, differentiate into immunosuppressive TAMs and MDSCs. Tumor-recruited myeloid cells have been shown to exert supportive tumor-promoting effects via multiple pathways that stimulate local immune suppression/tolerance, tumor angiogenesis, tissue remodeling, and cancer inflammation. However, their role in the degradation of extracellular HA and, particularly, of tumor-associated HA has not been recognized yet. We identified the myeloid cell subset within bladder cancer tissue that expresses the HA degrading Hyal2, suggesting involvement of these cells in the enhanced fragmentation of extracellular HA observed in tumor tissue. The increased presence of Hyal2-expressing myeloid cells was also detected in the peripheral blood of patients with bladder cancer. The HA-degrading function of Hyal2-expressing myeloid cell could be enhanced by exposure to the TCM, and IL1β was identified as one of the factors stimulating the Hyal2 activity. CD44-mediated signaling plays an important role in the regulation of HA-degrading activity of myeloid cells because stimulation of CD44 receptor with specific mAb triggered secretion of IL1β and translocation of Hyal2 to the cellular surface. Collectively, this work identifies the Hyal2-expressing myeloid cells and links these cells to the accumulation of LMW-HA in the tumor microenvironment.

## Authors' Disclosures

S. Kusmartsev reports a patent for Identification of tumor-associated Hyal2-expressing myeloid cells: novel target for cancer immunotherapy issued. No disclosures were reported by the other authors.

## Authors' Contributions

**P.R. Dominguez-Gutierrez:** Formal analysis, validation, investigation, visualization, methodology. **E.P. Kwenda:** Formal analysis, investigation. **W. Donelan:** Investigation, methodology. **P. O'Malley:** Resources. **P.L. Crispen:** Resources, supervision, writing-original draft. **S. Kusmartsev:** Conceptualization, resources, data curation, supervision, funding acquisition, methodology, writing-original draft, project administration, writing-review and editing.

## Acknowledgments

This work is supported by grant #8JK05 from J&E King Biomedical Research Program and Fund 1923 (to S. Kusmartsev).

The costs of publication of this article were defrayed in part by the payment of page charges. This article must therefore be hereby marked *advertisement* in accordance with 18 U.S.C. Section 1734 solely to indicate this fact.

Received April 11, 2020; revised November 17, 2020; accepted November 20, 2020; published first November 25, 2020.

## References

1. Girish KS, Kemparaju K. The magic glue hyaluronan and its eraser hyaluronidase: a biological overview. Life Sci 2007;80:1921–43.
2. Toole BP. Hyaluronan: from extracellular glue to pericellular cue. Nat Rev Cancer 2004;4:528–39.
3. Sironen RK, Tammi R, Tammi PK, Auvinen P, Anttila M, Kosma VM. Hyaluronan in human malignancies. Exp Cell Res 2011;317:393–91.
4. Simpson MA, Lokeshwar VB. Hyaluronan and hyaluronidase in genitourinary tumors. Front Biosci 2008;13:5664–80.
5. Schmaus A, Bauer J, Sleeman JP. Sugars in the microenvironment: the sticky problem of HA turnover in tumors. Cancer Metastasis Rev 2014;33: 1059–79.
6. Turley EA, Wood DK, McCarthy JB. Carcinoma cell hyaluronan as a "portable" cancerized pro-metastatic microenvironment. Cancer Res 2016; 76:2507–12.
7. Tian X, Azpurua J, Hine C, Vaidya A, Myakishev-Rempel M, Ablaeva J, et al. High-molecular-mass hyaluronan mediates the cancer resistance of the naked mole rat. Nature 2013;499:346–49.
8. Ooki T, Murata-Kamiya N, Takahashi-Kanemitsu A, Wu W, Hatakeyama M. High-molecular-weight hyaluronan is a hippo pathway ligand directing cell density-dependent growth inhibition via PAR1b. Dev Cell, 2019;49: 590–604.
9. Sokolowska M, Chen LY, Eberlein M, Martinez-Anton A, Liu Y, Alsaaty S, et al. . Low molecular weight hyaluronan activates cytosolic phospholipaseA2α and eicosanoid production in monocytes and macrophages. J Biol Chem 2014;289: 4470–88.
10. Kramer MW, Golshani R, Merseburger AS, Knapp J, Garcia A, Hennenlotter J, et al. HYAL-1 hyaluronidase: A potential prognostic indicator for progression to muscle invasion and recurrence in bladder cancer. Eur Urol 2010; 57:86–94.
11. Van Der Heijden AG, Mengual L, Lozano JJ, Ingelmo-Torres M, Ribal M, Fernandez PL, et al. A five-gene expression signature to predict progression in T1G3 bladder cancer. Eur J Cancer 2016;64:127–36.
12. Stern R. Hyaluronidases in cancer biology. Semin Cancer Biol 2008;18: 275–80.
13. Harada H, Takahashi M. CD44-dependent intracellular and extracellular catabolism of hyaluronic acid by hyaluronidase-1 and -2. J Biol Chem 2007; 282:5597–607.
14. Eruslanov E, McCullers M, Daurkin I, Algood C, Dahm P, Rosser CJ, et al. Circulating and tumor-infiltrating myeloid cell subsets in patients with bladder cancer. Int J Cancer 2012;130:1109–19.
15. Takeyama Y, Kato M, Tamada S, Azuma Y, Shimizu Y, Iguchi T, et al. Myeloid-derived suppressor cells are essential partners for immune checkpoint inhibitors in the treatment of cisplatin-resistant bladder cancer. Cancer Lett 2020;479:89–99.
16. Petrey AC, De la Motte CA. Thrombin cleavage of inter-α-inhibitor heavy chain 1 regulates leukocyte binding to an inflammatory hyaluronan matrix. J Biol. Chem. 2016;291:24324–34.
17. Min H, Cowman MK. Combined alcian blue and silver staining of glycosaminoglycans in polyacrylamide gels: application to electrophoretic analysis of molecular weight distribution. Anal Biochem 1986;155: 275–85.
18. Daurkin I, Eruslanov E, Stoffs T, Perrin GQ, C. Algood G, Gilbert SM, et al. Tumor-associated macrophages mediate immune suppression in kidney cancer microenvironment by activating 15-lipoxygenase pathway. Cancer Res 2011;71: 6400–9.
19. Prima V, Kaliberova L, Kaliberov S, Curiel D, Kusmartsev S. COX2-mPGES1-$PGE_2$ pathway regulates PD-L1 expression in tumor-associated macrophages and myeloid-derived suppressor cells. Proc Natl Acad Sci U S A 2017;114:1117–22.
20. Biswas SK, Mantovani A.. Macrophage plasticity and interaction with lymphocyte subsets: cancer as a paradigm. Nat Immunol 2010;11:889–96.
21. Gabrilovich DI, Ostrand-Rosenberg S, Bronte V. Coordinated regulation of myeloid cells by tumours. Nat Rev Immnil 2012;12:253–68.
22. Crispen PL, Kusmartsev S. Mechanisms of immune evasion in bladder cancer. Cancer Immunol Immunother 2020;69:3–14.
23. Bourguignon LY, Singleton PA, Diedrich F, Stern R, Gilad E. CD44 interaction with Na+-H+ exchanger (NHE1) creates acidic microenvironments leading to hyaluronidase-2 and cathepsin B activation and breast tumor cell invasion. J Biol Chem 2004;279:26991–7007.
24. Duterte C, Mertens-Strijthagen J, Tammi M, Flamion B. Two novel functions of hyaluronidase-2 (Hyal2) are the formation of the glycocalyx and control of CD44-ERM interactions. J Biol Chem 2009;284:33495–508.
25. Jang JH, Kim DH, Lim JM, Lee JW, Jeong SJ, Kim KP, et al. Breast cancer cell-derived soluble CD44 promotes tumor progression by triggering macrophage IL1b production. Cancer Res 2020;80:1342–956.
26. Jiang D, Liang J, Noble PW. Hyaluronan as an immune regulator in human diseases. Physiol Rev 2011;91:221–64.
27. Cnanmee T, Ontong P, Itano N. Hyaluronan: A modulator of the tumor microenvironment. Cancer Lett 2016;375:20–30.
28. Jiang D, Liang J, Fan J, Yu S, Chen S, Luo Y, et al. Regulation of lung injury and repair by toll-like receptors and hyaluronan. Nat Med, 2005;11:1173–9.
29. Voelcker V, Gebhardt C, Averbeck M, Saalbach A, Wolf V, Weih F, et al. Hyaluronan fragments induce cytokine and metalloprotease upregulation in human melanoma cells in part by signalling via TLR4. Exp Dermatol 2008;17: 100–7.
30. West DC, Hampson IN, Arnold F, Kumar S. Science 1985;228:1324–6.
31. Matou-Nasri S, Gaffney J, Kumar S, Slevin M. Oligosaccharides of hyaluronan induce angiogenesis through distinct CD44 and RHAMM-mediated signalling pathways involving Cdc2. Int J Oncol 2009;35:761–73.
32. Gao F, Liu Y, He Y, Yang C, Wang Y, Shi X, et al. Hyaluronan oligosaccharides promote excisional wound healing through enhanced angiogenesis. Matrix Biology: J Int Society Matrix Biol 2010;29:107–16.
33. Itano N, Sawai T, Miyaishi O, Kimata K. Relationship between hyaluronan production and metastatic potential of mouse mammary carcinoma cells. Cancer Res 1999;59:2499–504.
34. Schmaus A., Klusmeier S., Rothley M., Dimmler A., Sipos B., Faller G., et al. Accumulation of small hyaluronan oligosaccharides in tumour interstitial fluid correlates with lymphatic invasion and lymph node metastasis. Br J Cancer 2014; 111:559–67.
35. Rai SK, Duh FM, Vigdorovich V, Danilkovitch-Miagkova A, Lerman MI, Miller AD. Candidate tumor suppressor HYAL2 is a glycosylphosphatidylinositol (GPI)-anchored cell-surface receptor for jaagsiekte sheep retrovirus, the envelope protein of which mediates oncogenic transformation. Proc Natl Acad Sci USA 2001;98:4443–8.
36. Andre B, Duterme C, Van Moer K, Mertens-Strijthagen J, Jadot M, Flamion B. Hyal2 is a glycosylphosphatidylinositol-anchored, lipid

raft-associated hyaluronidase. Biochem Biophys Res Commun 2011;411: 175–9.
37. Stern R. Devising a pathway for hyaluronan catabolism: are we there yet. Glycobiology 2003;13:105–15.
38. Czoka AB, Frost GI, Stern R. The six hyaluronidase-like genes in the human and mouse genomes. Matrix Biol, 200120:499–508.
39. Stern R. Hyaluronan metabolism: a major paradox in cancer biology. Pathol Biol (Paris) 2005;53:372–82.
40. Yoshida M, Sai S, Marumo K, Tanaka T, Itano N, Kimata K, et al. Expression analysis of three isoforms of hyaluronan synthase and hyaluronidase in the synovium of knees in osteoarthritis and rheumatoid arthritis by quantitative real-time reverse transcriptase polymerase chain reaction. Arthritis Res. Ther 2004;6:R514–R20.
41. Tanimoto K, Yanagida T, Tanne Y, Kamyaa T, Huang YC, Mitsuyoshi T, et al. Modulation of hyaluronan fragmentation by interleukin-1beta in synovial membrane cells, Ann Biomed Eng 2010;38:1618–25.
42. Kaplanov I, Carmi Y, Kornetsky R, Shemesh A, Shurin GV, Shurin MR, et al. Blocking IL-1β reverses the immunosuppression in mouse breast cancer and synergizes with anti-PD-1 for tumor abrogation. Proc Natl Acad Sci USA 2019; 116:1361–69.